Monte Carlo simulation of the nematic-isotropic transition in an isothermal-isobaric ensemble

Abhijit Pal and Soumen Kumar Roy
Department of Physics, Jadavpur University, Calcutta 700032, India
(Received 25 April 2003; revised manuscript received 22 September 2003; published 27 February 2004)

Monte Carlo simulation of a system consisting of 512 cylindrically symmetric particles interacting with each other via a potential which has an isotropic, density dependent part as well as an anisotropic part has been used to simulate the nematic state. The usual Metropolis algorithm is used and the particles are allowed to have translational degrees of freedom along with the orientational one. The simulation has been carried out in an isothermal-isobaric (NPT) ensemble and the multiple histogram technique of Ferrenberg-Swendsen with appropriate modification for the NPT ensemble has been used. The results reveal realistic values of the pseudospinoidal temperature and pressure as well as that for the pressure dependence of the nematic-isotropic transition temperature.

DOI: 10.1103/PhysRevE.69.021709 PACS number(s): 61.30.Cz, 64.70.Md, 87.53.Wz

I. INTRODUCTION

The Maier-Saupe (MS) model [1] of nematic liquid crystals has been successful in explaining the basic features of the nematic-isotropic phase transition. The Lebwohl-Lasher (LL) model [2] is the lattice version of the MS model where the cylindrically symmetric particles are confined to the sites of a cubic lattice and interact with the nearest neighbors with the Hamiltonian given by

$$H = -\epsilon \sum_{i,j} P_2(\cos\theta_{ij}), \tag{1}$$

where P_2 is the second Legendre polynomial and θ_{ij} is the angle between the symmetry axes of the molecules at the nearest neighbor sites i and j. The quantity ϵ is a strength factor. The LL model does not take into account the coupling between the translational and the rotational degrees of freedom between the molecules which is always present in a real nematic. In spite of this shortcoming, the LL model has been investigated by a number of researchers. Fabbri and Zannoni [3] have performed Monte Carlo (MC) simulation in this model for a lattice size up to 30^3. Subsequently Zhang *et al.* [4] investigated system size up to 28^3 using this model and have performed finite size scaling to determine the thermodynamic limit of the transition temperature. More recently Priezjev and Pelcovits [5] worked on lattice of size up to 70^3 which vastly improved the statistics of the finite size scaling they performed.

One puzzling aspect of the nematic-isotropic (NI) transition has been the smallness of the quantity $|(T^- - T_c)|/T_c$, where T_c is the NI transition temperature and T^- is the limit of supercooling of the isotropic liquid. Experimentally one observes this quantity to be $\sim$0.1% while the theoretical predictions [1] have been one or more orders of magnitude higher. Zhang *et al.* [4] in their simulation on the LL model have estimated that this quantity is $\leqslant$0.5% which may be termed moderately good. No estimate of this quantity is however available from the work of Priezjev and Pelcovits [5].

Tao *et al.* [6] reported a work on an extended mean-field theory of the nematic-isotropic transition. These authors took into consideration an isotropic, density dependent component of the molecular interaction. This is an improvement over the MS theory which considers only the orientational part of the interaction between the molecules and hence is unable to predict the density variation observed at the NI transition. Also no change in T_c with pressure, which is easily observed experimentally, is either explainable in terms of the MS theory. The inclusion of the density dependent, isotropic interaction in the nematic Hamiltonian resulted in great improvement in the predicted value of $|(T^- - T_c)|/T_c$ and the right magnitude of the density variation at T_c. Also the theory resulted in a realistic prediction of the quantity dT_c/dP, where P is the pressure. It may be noted that these improvements were made while still working within the framework of the mean-field theory where the fluctuations in the neighborhood of T_c do not play a dominant role.

One motivation behind the present work has been to perform MC simulation by including an isotropic, density dependent term in the Hamiltonian besides the usual anisotropic interaction where the particles are not fixed in any lattice and are allowed to have translational degrees of freedom. One can then see directly, without the approximations intrinsic in the mean-field theory, the effect of inclusion of the isotropic part of the interaction on the different features of the nematic isotropic transition. For this purpose we have performed MC simulation in an isothermal-isobaric ensemble (*NPT* ensemble) instead of the usual *NVT* (canonical) ensemble. This closely resembles the general experimental situation where the pressure is kept constant and the volume is allowed to change freely. More than two decades ago Luckhurst and Romano [7] performed an NPT MC simulation in a system consisting of 256 cylindrically symmetric particles with an isotropic part included in the potential which also consisted of an anisotropic part. The particles were not confined to a lattice and were allowed to have translational displacements in addition to the orientational one. Although the statistics of the work was not very good the simulation exhibited a weakly first order nematic isotropic transition.

We have performed the NPT MC simulation in a system consisting of 512 particles where each particle was allowed to interact with all other particles. The particles were allowed

to have translational degrees of freedom in addition to the usual orientational one. Although our system size is not very large, the work involved a considerable amount of computation as large number of interactions had to be taken care of and we have applied the multiple histogram reweighing technique which was first suggested by Ferrenberg and Swendsen [8]. The method had to be slightly modified so as to enable us to work in a NPT ensemble and the details are provided in the following sections. Actually our work which is an elaborated example of the application of multiple histogram reweighing in a NPT ensemble, may be extended to perform more extensive and useful work in similar or other systems. This is the other motive behind the present work.

II. THE POTENTIAL USED IN THE PROBLEM AND DEFINITION OF RELATED THERMODYNAMIC QUANTITIES

Monte Carlo simulation was performed in a system consisting of 512 particles using the usual Metropolis algorithm [9]. The potential used is of the form

$$U = U_0 + U_a, \tag{2}$$

where U_0 is the isotropic part of the interaction and is nothing but a Lennard-Jones (LJ) potential which can be written as

$$U_0(r_{ij}) = 4\epsilon\{(\sigma/r_{ij})^{12} - (\sigma/r_{ij})^6\}, \tag{3}$$

where r_{ij} is the intermolecular separation between the ith and jth particles respectively, σ being the separation where U_0 vanishes and ϵ is the strength parameter. The anisotropic part of the potential is taken as

$$U_a = -4\lambda\epsilon(\sigma/r_{ij})^6 P_2(\cos\theta_{ij}), \tag{4}$$

where $P_2(\cos\theta_{ij})$ is the second Legendre polynomial, θ_{ij} being the angle between the symmetry axes of the ith and jth particles, λ is the anisotropic parameter whose value is chosen to be 0.15. Such a value of λ has been found to be optimum because smaller values of λ does not give rise to a liquid crystalline phase above the melting point and for higher values an orientationally ordered phase is stable up to the boiling point [7]

We define the reduced internal energy per particle E^* and the reduced enthalpy per particle H^* as

$$E^* = E/N\epsilon, \tag{5}$$

$$H^* = E^* + P^*V^*, \tag{6}$$

where $P^*(=P\sigma^3/\epsilon)$ and $V^*(=V/N\sigma^3)$ are the reduced pressure and reduced volume, respectively. ϵ and σ are the parameters which appear in the Lennard-Jones potential of Eq. (3). The specific heat per particle at constant pressure is given by

$$C_P^* = \frac{d}{dT^*}\langle H^*\rangle, \tag{7}$$

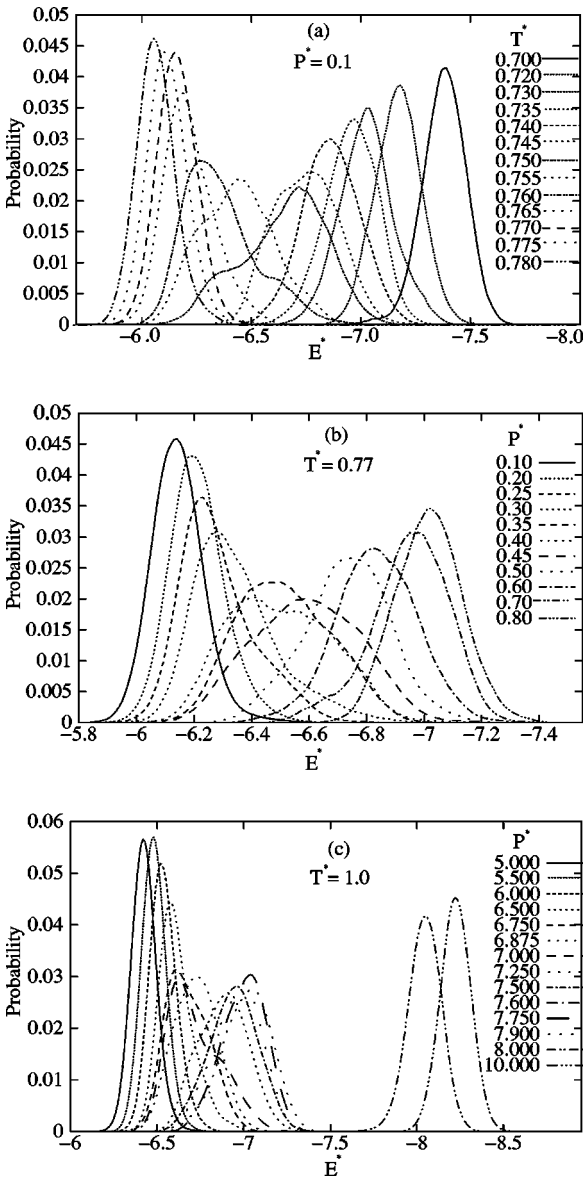

FIG. 1. Histograms for reduced energy obtained in simulations (i), (ii), and (iii), respectively.

which can also be evaluated from fluctuation as

$$C_P^* = \frac{(\langle H^{*2}\rangle - \langle H^*\rangle^2)}{T^{*2}} \tag{8}$$

where $T^*(=kT/\epsilon)$ is the reduced temperature.

The isothermal compressibility is given by

$$K_T^* = -\frac{1}{V^*}\frac{d}{dT}\langle V^*\rangle. \tag{9}$$

The conventional long range order parameter is given by

$$\langle P_2\rangle = \tfrac{1}{2}\langle 3\cos^2\theta - 1\rangle, \tag{10}$$

where θ is the angle that a molecular symmetry axis makes with the preferred direction of orientation which was ob-

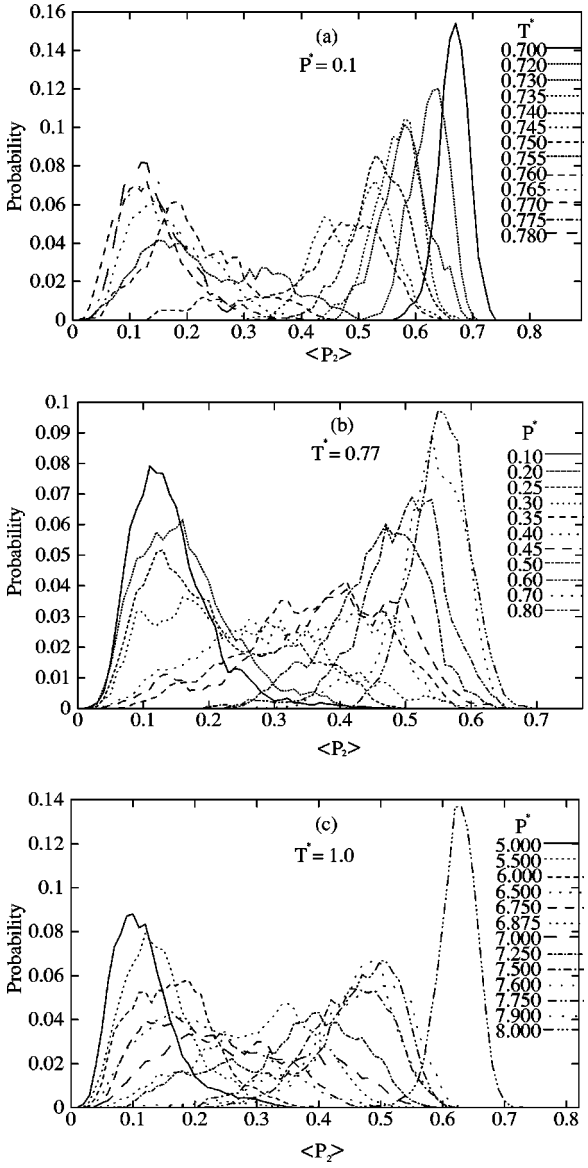

FIG. 2. Order parameter histograms for simulations (i), (ii), and (iii), respectively.

tained by maximizing $\langle P_2 \rangle$ [3] and the average is over the entire sample. The order parameter susceptibility is defined in terms of the fluctuations of the order parameter $\langle P_2 \rangle$ as

$$\chi_0 = \frac{(\langle P_2^2 \rangle - \langle P_2 \rangle^2)}{T^*}. \tag{11}$$

The second rank angular correlation function is given by

$$G_2(r_{ij}) = \langle P_2(\cos\theta_{ij}) \rangle_{r_{ij}}, \tag{12}$$

where θ_{ij} is the angle between the symmetry axes between the ith and jth particles separated by a distance r_{ij}. The radial distribution function [10] $g(r)$ is defined as the probability of finding a pair of particles at a distance r apart, relative to the probability expected for a completely random distribution at the same density. It is nothing but the number of atoms a distance r apart from a given atom compared with the number at the same distance in an ideal gas at the same density.

TABLE I. The autocorrelation times (in number of MC sweeps) for reduced energy (E^*), order parameter ($\langle P_2 \rangle$) and (V^*) for all temperatures and pressures.

			$P^*=0.1$				
T^*	0.700	0.720	0.730	0.735	0.740	0.745	0.75
$\tau(E^*)$	2385	3006	6555	8163	8550	14522	28117
$\tau(\langle P_2 \rangle)$	3602	4855	9456	10336	11994	18065	38337
$\tau(V^*)$	1800	2288	4564	6453	7867	9950	15986
T^*	0.755	0.760	0.765	0.770	0.775	0.780	
$\tau(E^*)$	23933	14578	6369	2166	1242	1011	
$\tau(\langle P_2 \rangle)$	29214	22653	13188	11142	8950	6859	
$\tau(V^*)$	11056	6739	4367	2706	1731	1235	
			$T^*=0.77$				
P^*	0.10	0.20	0.25	0.30	0.35	0.40	
$\tau(E^*)$	2166	8127	25342	49253	63284	31466	
$\tau(\langle P_2 \rangle)$	11142	19272	38416	64453	78731	41825	
$\tau(V^*)$	527	933	5282	11673	26835	18290	
P^*	0.45	0.50	0.60	0.70	0.80		
$\tau(E^*)$	20167	16686	14147	13186	6618		
$\tau(\langle P_2 \rangle)$	29632	19613	18584	17180	8194		
$\tau(V^*)$	10617	7268	5725	3914	1104		
			$T^*=1.0$				
P^*	5.000	5.500	6.000	6.500	6.750	6.875	
$\tau(E^*)$	1102	1419	3135	10451	11880	12725	
$\tau(\langle P_2 \rangle)$	3593	5784	8610	15047	16235	17659	
$\tau(V^*)$	423	746	1178	2039	3157	5294	
P^*	7.000	7.250	7.500	7.600	7.750	7.900	
$\tau(E^*)$	13946	11025	8983	7013	5930	5260	
$\tau(\langle P_2 \rangle)$	18497	14872	11345	10024	9047	8161	
$\tau(V^*)$	9846	7102	4672	4103	3100	2478	

III. COMPUTATIONAL DETAILS

In the simulation we have performed in an isothermal-isobaric (NPT) ensemble, the number of particles N, pressure P and temperature T were kept fixed and the volume V of the system was allowed to change. Thus N particles are placed in a cubic cell with the values of pressure and temperature assigned. The configurational average of an observable A is given by

$$\langle A \rangle = \frac{\int_0^\infty dV \exp(-\beta PV) V^N \int d\vec{r}\, A(\vec{r}) \exp(-\beta U(\vec{r}))}{Z}, \tag{13}$$

where Z is the configurational part of the partition function which can be written as

$$Z = \int dV \exp(-\beta PV) \int d\vec{r} \exp[-\beta U(\vec{r})], \tag{14}$$

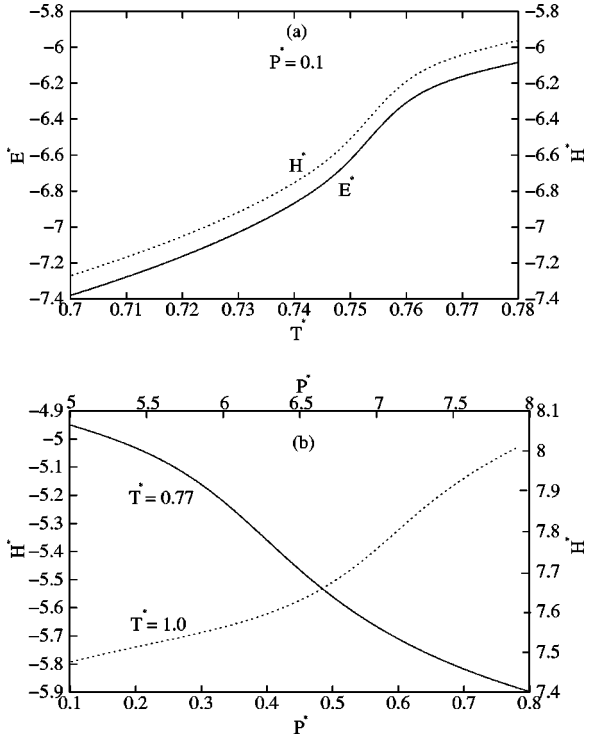

FIG. 3. Reweighed values of reduced energy and reduced enthalpy for the simulations indicated. In (b) the lower scale and the scale on the left correspond to $T^*=0.77$ and the top scale and the right scale correspond to $T^*=1.0$.

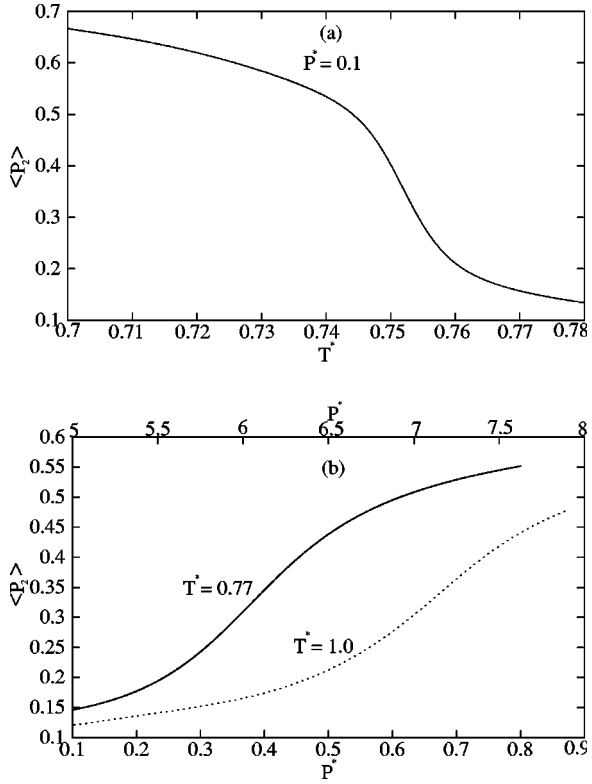

FIG. 4. Reweighed values of order parameter for the simulations indicated. In (b) the lower scale and the top scale correspond to $T^*=0.77$ and $T^*=1.0$, respectively.

where $\beta=1/K_BT$, K_B is Boltzmann's constant, V is the volume and U is the potential energy of the system.

The Metropolis algorithm is followed by generating a Markov chain in which a new state is generated by giving a particle a random translational and orientational displacement along with a volume change by changing the box length randomly [10]. The changes in the box length is given by

$$L_n=L_m+\delta l_{max}(2\xi_L-1). \tag{15}$$

The positional coordinates are then scaled according to the prescription given by

$$\vec{r}_{i,n}=\vec{r}_{i,m}L_n/L_m, \tag{16}$$

where $i=1,512$. Changes in the positional coordinates of the ith particle while going from the nth state to the kth state are given by the prescription

$$\vec{r}_{i,k}=\vec{r}_{i,n}+\delta r_{max}(2\vec{\xi}_i-1). \tag{17}$$

While the changes in the orientational coordinates are given by

$$\vec{e}_{i,k}=\vec{e}_{i,m}+\delta\theta_{max}(2\vec{\xi}_i-1) \tag{18}$$

where the components of $\vec{e}_i$ are the normalized direction cosines and those of $\vec{\xi}_i$ are the random numbers in the interval (0,1). The values of δr_{max}, $\delta\theta_{max}$ and δl_{max} are chosen so as to make the acceptance-rejection ratio of the moves nearly equal. The enthalpy change in moving from the mth state to the kth state, δH_{km}, is given by

$$\delta H_{km}=\delta U_{km}+P(V_k-V_m)-N\beta^{-1}ln(V_k/V_m) \tag{19}$$

while the moves are accepted with a probability equal to $\min[1,\exp(\beta\delta H_{km})]$.

Initially the 512 particles were placed on the sites of a simple cubic lattice, interacting through purely LJ potential [Eq. (3)] and the reduced pressure P^* was set at 0.1. Each particle in the box is allowed to interact with every other particle. A move was considered as the change in the particle coordinates along with with the change in the box length. Metropolis algorithm was followed along with periodic boundary conditions and minimum image conventions [10]. Initially the system was heated to $T^*=3.0$ and about 10^6 configurations per particle were generated for equilibration and to make the centers of mass of the particles random. The anisotropic part [Eq. (4)] was added to the pure LJ interaction, keeping the symmetry axes of all the particles parallel. The nematic sample was cooled to $T^*=0.7$ and an equilibration run of length 10^7 configurations per particle was taken. Then the system was heated in steps up to $T^*=0.78$ and equilibration runs of about same length were taken for each temperature. The starting configuration for each temperature was taken from the final configuration of preceding lower temperature. The histograms for energy, order parameter and volume were generated for each temperature.

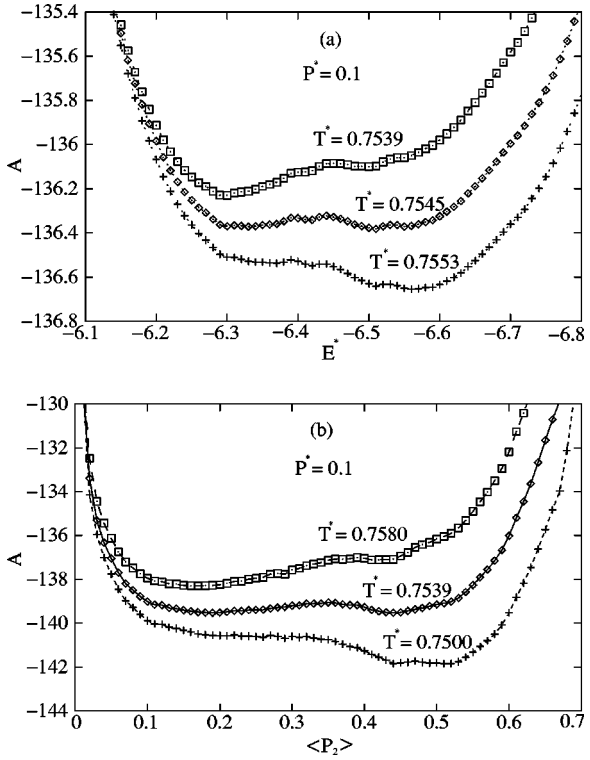

FIG. 5. The free energy A plotted against reduced energy and order parameter in simulation (i).

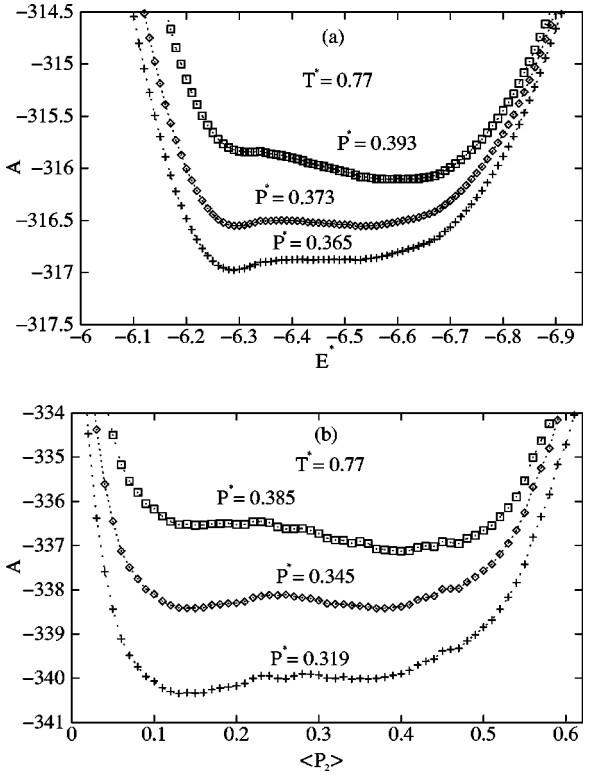

FIG. 6. The free energy A plotted against reduced energy and order parameter in simulation (ii).

The MC simulations for pressure variation were performed for two sets of temperatures. First, keeping the reduced temperature $T^*=0.77$ fixed, the reduced pressure was increased from $P^*=0.1$ to $P^*=0.8$. The system was then heated to a higher temperature $T^*=1.0$ and keeping the temperature $T^*=1.0$ of the system fixed the reduced pressure was increased from $P^*=5.0$ to $P^*=10.0$. In both cases equilibration runs of length 10^7 configurations per particle were taken and for each pressure histograms for energy, order parameter and volume were generated. The starting configurations at each pressure were taken from the final configurations of the preceding lower pressure.

The various thermodynamic quantities were computed using the histogram reweighing technique of Ferrenberg and Swendsen [8]. In this work we have applied the above mentioned technique for the process involving temperature variation at a fixed pressure as well as the reverse process. We summarize below the essential equations for the evaluation of various averages in our simulation.

In case of temperature variation where the pressure of the system is kept unchanged, suppose that R Monte Carlo simulations have been performed at temperatures $K_n, n=1,\ldots,R$ and the data has been stored as histograms $\{N_n(E,V)\}$, with the total number of configurations is $n_n=\Sigma_{n=1}^{R}N_n$. We define a quantity $g_n=1+2\tau_n$, where τ_n is the autocorrelation time and $K=-1/T$ where we have set the Boltzmann constant equal to 1. Then the essential multiple histogram equation for the probability $p(E,V,K)$ is written as

$$p(E,V,K)=\frac{\sum_{n=1}^{R} g_n^{-1}N_n(E,V)\exp[K(E+PV)]}{\sum_{m=1}^{R} n_m g_m^{-1}\exp[K_m(E+PV)-f_m]}, \quad (20)$$

where the free energy f_n is given by

$$\exp\{f_n\}=\sum_E \sum_V p(E,V,K_n) \quad (21)$$

the values of f_n could be obtained self-consistently by iterating Eq. (20) and (21). Either $p(E,K)$ or $p(V,K)$ can now be obtained by summing $p(E,V,K)$ over V or E, respec-

TABLE II. Pseudospinoidal temperatures and pressures obtained from energy and order parameter data for simulation (i) and (ii).

$P^*=0.1$		
T	from f vs E^*	from f vs $\langle P_2\rangle$
T_c	0.7545	0.7539
T^+	0.7553	0.7580
T^-	0.7539	0.7500
$T^*=0.77$		
P	from f vs E^*	from f vs $\langle P_2\rangle$
P_c	0.373	0.345
P^+	0.393	0.385
P^-	0.365	0.319

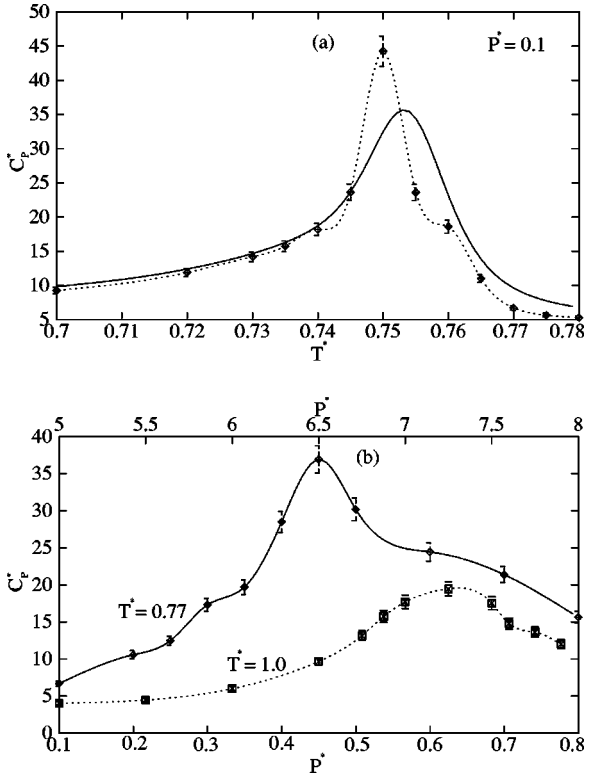

FIG. 7. The specific heat at constant pressure plotted against (a) temperature and (b) pressure. In (a) the solid line represents the C_P^* obtained from dH^*/dT^* and the dashed curve is the same obtained from fluctuations in enthalpy. In (b) the solid curve which represents the C_P^* for $T^*=0.77$ has the pressure given by the lower scale while the dashed curve for $T^*=1.0$ has the pressure given by the upper scale.

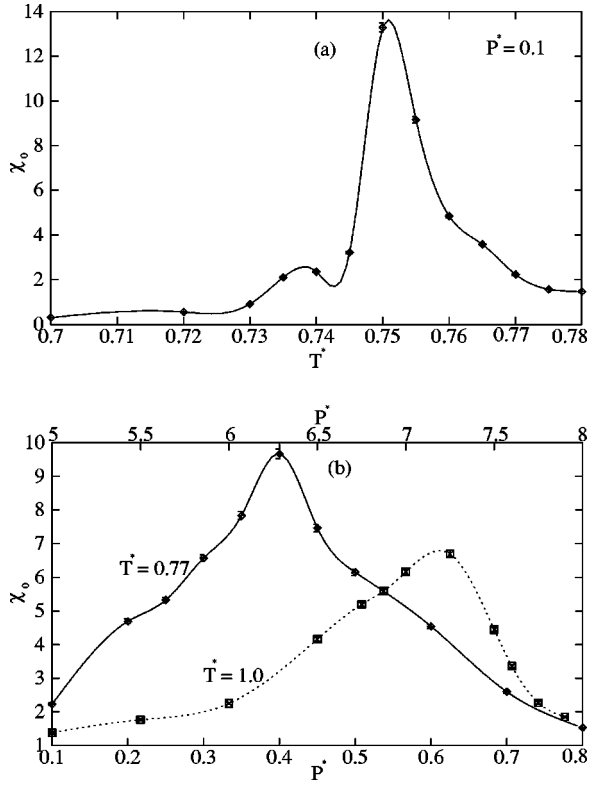

FIG. 8. The order parameter susceptibility χ_0 plotted against (a) temperature and (b) pressure. In (b) the lower scale is for $T^*=0.77$ and the top one is for $T^*=1.0$.

tively, and the average value of any operator on E and V can accordingly be evaluated as a function of K.

In order to apply the multiple histogram reweighing technique in case of the determination of the order parameter $\langle P_2\rangle$ the essential multiple histogram equation can be modified as

$$p(E,V,\langle P_2\rangle,K)=\frac{\sum_{n=1}^{R} g_n^{-1}N_n(E,V,\langle P_2\rangle)\exp[K(E+PV)]}{\sum_{m=1}^{R} g_m^{-1}\exp[K_m(E+PV)-f_m]}, \tag{22}$$

where the free energy f_n is given as

$$\exp\{f_n\}=\sum_E \sum_V \sum_{\langle P_2\rangle} p(E,V,\langle P_2\rangle,K_n) \tag{23}$$

As above $p(\langle P_2\rangle,K)$ can be obtained by summing $p(E,V,\langle P_2\rangle,K)$ over E and V.

In case of pressure variation where the temperature of the system is kept constant, R' Monte Carlo simulations have been performed at different pressures $P_{n'}, n'=1,\ldots,R'$.

For the determination of the order parameter the essential multiple histogram equation can be written as

$$p(E,V,\langle P_2\rangle,P)=\frac{\sum_{n'=1}^{R'} g_{n'}^{-1}N_{n'}(E,V,\langle P_2\rangle)\exp[K(PV)]}{\sum_{m'=1}^{R'} n_{m'}g_{m'}^{-1}\exp[K(P_{m'}V)-f_{m'}]}, \tag{24}$$

where the free energy $f_{n'}$ is given as

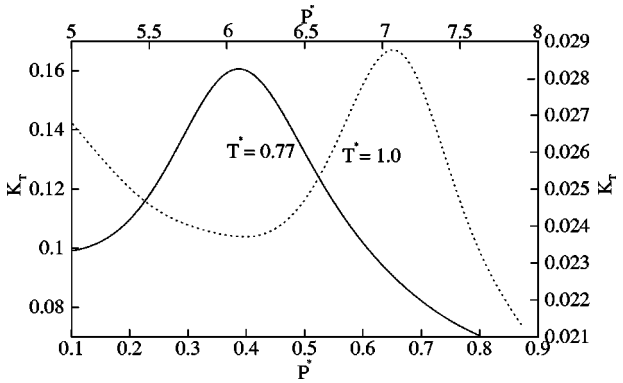

FIG. 9. The isothermal compressibility K_T plotted against pressure. The lower scale and the scale on the left correspond to $T^*=0.77$ and the top scale and right scale correspond to $T^*=1.0$.

TABLE III. Transition temperatures and pressures obtained by different methods.

$P^*=0.1$				
dH^*/dT^*	C_P^* (fluctuation)	χ_0	$d\langle P_2\rangle/dT^*$	
T_c	0.7530	0.7501	0.7509	0.7520
	$T^*=0.77$			
C_P^* (fluctuation)	χ_0	K_T		
P_c	0.454	0.397	0.388	
	$T^*=1.0$			
C_P^* (fluctuation)	χ_0	K_T		
P_c	7.314	7.197	7.070	

$$\exp\{f_{n'}\}=\sum_E \sum_V \sum_{\langle P_2\rangle} p(E,V,\langle P_2\rangle,P_{n'}). \qquad (25)$$

IV. RESULT AND DISCUSSION

The Monte Carlo simulations we have performed essentially consist of three parts. In the first part (i) the reduced pressure was kept fixed at $P^*=0.1$ and the reduced temperature was varied from $T^*=0.70$ to 0.78. In all 13 temperatures were used for simulations in this range. The second (ii) and the third (iii) parts of the simulation involve variation of pressure keeping the temperature fixed at $T^*=0.77$ and 1.0, respectively. The pressure was varied in the ranges 0.1 to 0.8 (11 values) and 5.0 to 7.9 (12 values), respectively. In each simulation the histograms were generated for the reduced energy E^*, the reduced volume V^* and the order parameter $\langle P_2\rangle$. In Figs. 1 and 2 some of these histograms are shown. Figure 1(a) displays the histograms for the set (i) where the pressure is held fixed at $P^*=0.1$ and the histograms in the neighborhood of $T^*=0.75$ show the evidence of sampling between two phases. The situation is similar for the histograms in Fig. 1(b) where the pressure is varied and the temperature is kept fixed at 0.77. Figure 1(c) shows the energy histograms for $T^*=1.0$ and we note here that there is a large gap for the pressure between 7.9 and 8.0 and the histograms for $P^*=8.0$ and 10.0 presumably represent the solidified phase which developed at high pressure. Figure 2(a) shows the order parameter histograms for $P^*=0.1$ where temperature is varied. Figures 2(b) and 2(c) again show the order parameter histograms for $T^*=0.77$ and $T^*=1.0$ and here pressure is the parameter which is varied.

In order to perform the multiple histogram reweighing, which we have already discussed in detail, it is necessary to determine the relevant auto-correlation times. We have determined these using the method outlined by Madras and Sokal [12] and the results are shown in Table I. Figure 3(a) and 3(b) show the reweighted energy E^* and the enthalpy H^* for the simulations (i), (ii), and (iii), respectively while those for the order parameter $\langle P_2\rangle$ are depicted in Figs. 4(a) and 4(b). The error in estimating the probability $p(S,K)$ in the histograms is given by

$$\delta p(S,K)=\left[\sum_n g_n^{-1}N_n(S)\right]^{-1/2} p(S,K), \qquad (26)$$

with S being an observable like the energy, order parameter, or the volume and $g_n=2\tau_n+1$, τ_n is the autocorrelation time for the nth simulation. These errors have a peak value $\sim$3% for Monte Carlo simulations (i) and (ii) and $\sim$1.5% for (iii). For the order parameter and volume histograms the errors are similar.

The free energy like quantity A which is equal to the negative logarithm of the probability $p(S)$ obtained from reweighing, was also determined. It is well known in the literature of the Monte Carlo simulation [11,13] that a double

TABLE IV. The transition temperature at different pressures obtained from the peak positions of the derivatives of enthalpy curves.

T^*	P^*
0.753	0.100
0.770	0.401
1.000	7.130

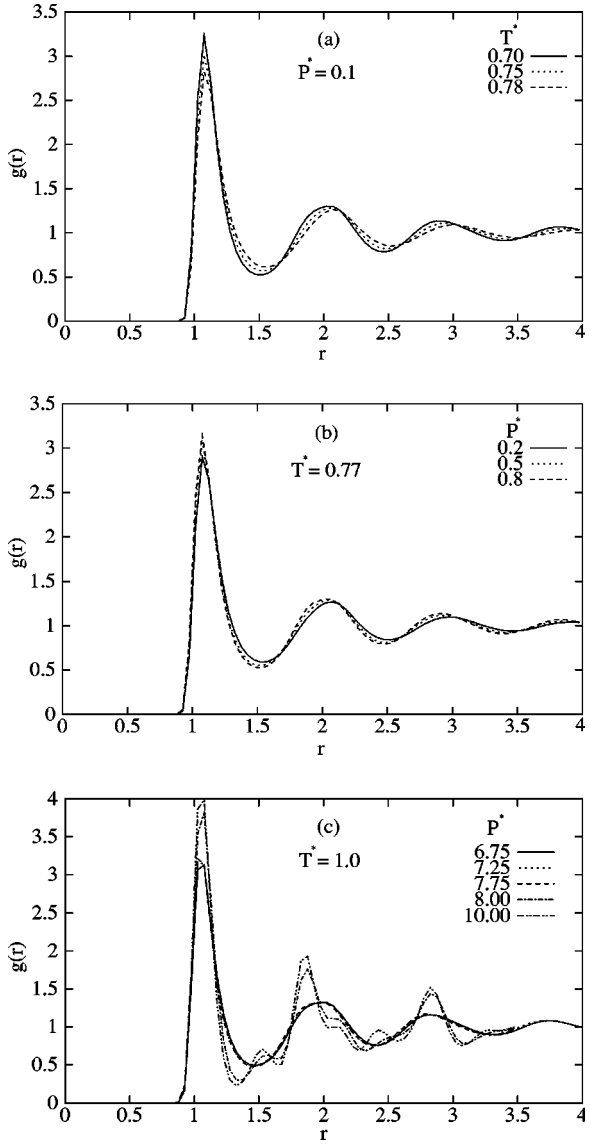

FIG. 10. The radial distribution function $g(r)$ for different temperatures and pressures.

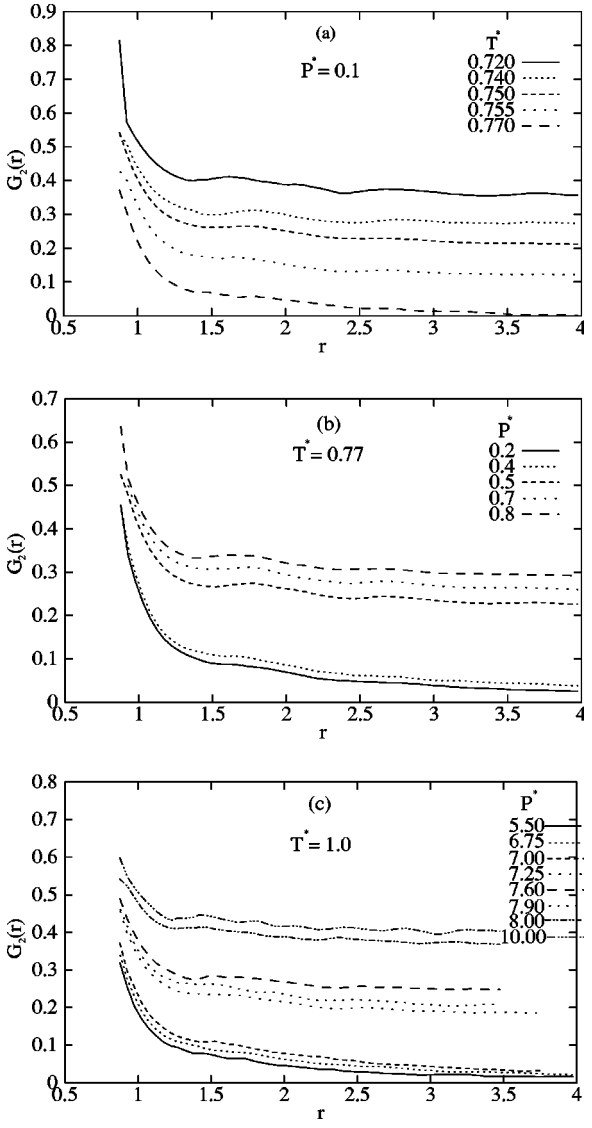

FIG. 11. The angular correlation function $G_2(r)$ plotted up to half the box length for a number of temperatures and pressures.

well structure of the quantity A characterizes a first order transition and the external parameters such as the temperature or pressure may be tuned to obtained the precise value of the parameter where a phase transition takes place. This occurs when the two wells in the free energy like quantity A are equally deep. Further information such as the pseudospinoidal temperature or pressure (as the case may be) may be obtained by fine tuning of the parameters so as to make one of the minima of A just disappear. In Figs. 5(a) and 5(b) we have shown the plots of the quantity A obtained from the energy and the order parameter histograms and have also determined the pseudospinoidal temperatures T^+ and T^-. In Figs. 6(a) and 6(b) are shown the identical quantities obtained from the energy and order parameter histograms and the transition pressure as well as the pseudospinoidal pressures were determined. The pseudospinoidal temperatures and pressures are listed in Table II.

The specific heat per particle at constant pressure C_P^* was determined from the temperature derivative of the enthalpy as well as from fluctuations of enthalpy and these are shown in Fig. 7(a). The peak positions which may be taken as the transition temperatures, $T_c=0.7501$ (fluctuation) and $T_c=0.7530$ (derivative), differ by about 0.4%, while the peak heights are not in good agreement with each other. The order parameter susceptibility χ_0 plotted against T^* for $P^*=0.1$ is shown in Fig. 8(a). The peak position of this suggests a transition temperature $T_c=0.7509$.

C_P^* obtained from fluctuation for $T^*=0.77$ and $T^*=1.0$ are shown in Fig. 7(b). The peak positions which indicate the respective transition pressures are given by $P_c=0.454$ and $P_c=7.314$, respectively. The order parameter susceptibility χ_0 for $T^*=0.77$ and $T^*=1.0$ plotted against pressure is shown in Fig. 8(b) and the transition pressures are given by $P_c=0.397$ and $P_c=7.197$, respectively. Finally the pressure variation of the isothermal compressibility K_T for these two temperatures are shown in Fig. 9 and these suggest the transition pressures to be $P_c=0.388$ and $P_c=7.070$, respectively. The transition temperatures and pressures are depicted in Table III. The significant difference in the transition pressures is believed to be due to finite size effects. It is expected that in the thermodynamic limit the differences in P_c^* obtained by different methods would tend to disappear.

We have evaluated $|(T^{\pm}-T_c)|/T_c$ from the knowledge of the values of the transition temperature. $|(T^+-T_c)|/T_c$ was found to be 0.1% and 0.5% for the temperatures determined from the energy and order parameter data while $|(T^- -T_c)|/T_c$ was found to be 0.08% and 0.5%, respectively. The MS theory, it may be recalled, yields values of these quantities to be $\sim$10% while the extended mean-field theory of Tao *et al.* gives $|(T^- -T_c)|/T_c \sim 0.1\%$. In a similar fashion we have also determined $|(P^{\pm}-P_c)|/P_c$ and these are 5.3% and 2.2% for energy data and 11.5% and 7.6% for the order parameter data respectively. To our knowledge, no experimental results are available for these quantities and we are thus unable to compare these with that happens in real systems. From the results shown in Table IV, we have estimated the pressure dependence of transition temperature. dT^*/dP^* turns out to be 0.0347, which when translated to dT/dP for N-c*p*-methoxybenzylidene-*p*-butylaniline (MBBA) (for which $\sigma \simeq 0.84\times 10^{-9}$ m), turns out to be $\sim$150 K/kbar. Although on the higher side this is of the same order of magnitude of what is found in most nematics viz 30−40 K/kbar.

The radial distribution function for simulations (i), (ii), and (iii) are shown in Fig. 10. It is evident from the results for $T^*=1.0$ that the peaks of $g(r)$ sharpen for $P^* \geqslant 8.0$ perhaps indicating solidification of the sample. The plots of the angular correlation function $G_2(r)$ for distances up to half the box length are shown in Fig. 11. In Figs. 11(b) and 11(c) it is seen that for low pressures $G_2(r)$ decays to zero indicating loss of long range order while the order increases with increase in pressure. For $T^*=1.0$ and $P^*=8.0$ and 10.0 the magnitude of $G_2(r)$ decreases very little and these pressures presumably characterize the solidified phase.

V. CONCLUSION

In the isothermal-isobaric simulation we have performed in the off-lattice model, which has closer resemblance with a

real nematic than the simple Lebwohl-Lasher model has, one would expect that the values of $|(T^{\pm}-T_c)|/T_c$ should be close to 0.1% as it happens in a real system. As we have already mentioned, in their MC simulation Zhang *et al.* [4] obtained values for these $\leqslant 0.5\%$ using the simple Lebwohl-Lasher model. Our results from energy data yield values of 0.1% and 0.08% for $|(T^{+}-T_c)|/T_c$ and $|(T^{-}-T_c)|/T_c$, respectively, which are good while those quantities evaluated from the order parameter give a somewhat higher value of 0.5% for both the quantities. This may perhaps be attributed to the small system size we have used. In order to test the finding of Tao *et al.* [6] that it is the density dependent term in the potential, rather than the fluctuations, which is responsible for the closeness of $T^{\pm}$ to T_c one must perform the simulation using the method described in this paper using bigger lattices and perhaps must do the finite size scaling in order to extract the thermodynamic limits of these quantities. It may however be pointed out in this context that Zhang *et al.* [4] got the above mentioned values of the pseudospinoidal temperatures by using lattices of size up to 28^3 and then performing finite size scaling. It may therefore be stated that the pseudospinoidal temperatures we obtained using a single lattice of relatively much smaller size indicate that the use of particles having translational degrees of freedom in the NPT ensemble is a far better approximation of a nematic than the Lebwohl-Lasher lattice model, as indeed it should.

We have thus demonstrated that the method of multiple histogram reweighing in an isothermal-isobaric ensemble can reveal a significant amount of information about the NI transition. But in view of the huge amount of CPU time involved, to extend this work to bigger systems, one would need to truncate the range of interaction and apply necessary corrections for that. This is however fairly straightforward and should not cause any problem.

ACKNOWLEDGMENT

We acknowledge the Computer Facility made available to us at the ICOSER Center (Level III Computer facility of DST) at the IACS, Calcutta.

[1] W. Maier and A. Saupe, Z. Naturforsch A, **13a**, 564 (1958); **14a**, 882 (1959); **15a**, 287 (1960).
[2] P.A. Lebwohl and G. Lasher, Phys. Rev. A **6**, 426 (1972).
[3] U. Fabbri and C. Zannoni, Mol. Phys. **58**, 763 (1986).
[4] Z. Zhang, O.G. Mouritsen, and M.J. Zuckermann, Phys. Rev. Lett. **69**, 2803 (1992).
[5] N.V. Priezjev and R.A. Pelcovits, Phys. Rev. E **63**, 062702 (2001).
[6] R. Tao, P. Sheng, and Z.F. Lin, Phys. Rev. Lett. **70**, 1271 (1993).
[7] G.R. Luckhurst and S. Romano, Proc. R. Soc. London, Ser. A **373**, 111 (1980).
[8] A.M. Ferrenberg and R.H. Swendsen, Phys. Rev. Lett. **61**, 2635 (1988); **63**, 1195 (1989).
[9] N. Metropolis, A.W. Rosenbluth, M.N. Rosenbluth, A.H. Teller, and E. Teller, J. Chem. Phys. **21**, 1087 (1953).
[10] *Computer Simulation of Liquids*, edited by M. P. Allen and D. J. Tildesley (Clarenden Press, Oxford, 1987).
[11] J. Lee and J.M. Kosterlitz, Phys. Rev. B **43**, 3265 (1991); Phys. Rev. Lett. **65**, 137 (1990).
[12] N. Madras and A.D. Sokal, J. Stat. Phys. **50**, 109 (1988).
[13] A. Pal and S.K. Roy, Phys. Rev. E **67**, 011705 (2003).